Bioorganic & Medicinal Chemistry 17 (2009) 7572–7584

Contents lists available at ScienceDirect

Bioorganic & Medicinal Chemistry

journal homepage: www.elsevier.com/locate/bmc

Synthesis and characterization of several carbamoyl- and methylcarbamoyl-substituted EMPO derivatives

Klaus Stolze [a,*], Natascha Rohr-Udilova [b], Andreas Hofinger [c], Thomas Rosenau [c]

[a] Molecular Pharmacology and Toxicology Unit, Department of Biomedical Sciences, University of Veterinary Medicine Vienna, Veterinärplatz 1, A-1210 Vienna, Austria
[b] Division of Gastroenterology and Hepatology, Department of Internal Medicine III, Medical University of Vienna, Währinger Gürtel 18-20, A-1090 Vienna, Austria
[c] Department of Chemistry, University of Natural Resources and Applied Life Sciences (BOKU), Muthgasse 18, A-1190 Vienna, Austria

ARTICLE INFO

Article history:
Received 20 April 2009
Revised 5 August 2009
Accepted 3 September 2009
Available online 6 September 2009

Keywords:
EPR
Spin trapping
Superoxide
EMPO
CAMPO/AMPO derivatives

ABSTRACT

The spin trapping behavior of four novel carbamoyl-substituted EMPO derivatives, namely 5-carbamoyl-3,5-dimethyl-pyrroline N-oxide (CADMPO), 3,5-dimethyl-5-methylcarbamoyl-pyrroline N-oxide (DMMCAPO), 5-carbamoyl-3-ethyl-5-methyl-pyrroline N-oxide (CAEMPO), and 3-ethyl-5-methyl-5-methylcarbamoyl-pyrroline N-oxide (EMMCAPO), towards different oxygen- and carbon-centered radicals is described, the half lives of the respective superoxide adducts ranging from about 10 to 20 min. The most characteristic adducts were, however, formed from methyl, hydroxymethyl, hydroxyethyl, and carbon dioxide anion radicals.

1. Introduction

Our previous studies have shown that the half lives of superoxide adducts of EMPO derivatives can be significantly increased if an ethyl or methyl substituent is present in position 3 or 4 of the pyrroline ring,[1–3] whereas the presence of a carbamoyl group in position 5 gives rise to secondary reactions of the spin trap, leading to the formation of 5-aminopyrroline derivatives in a Hofmann rearrangement reaction.[4] Additional complications arise due to the fact that different stereoisomers are formed due to the presence of two or more asymmetric carbon centers, exhibiting significantly different spin trapping properties and spin adduct stabilities (e.g., *cis*- and *trans*-3,5-EDPO/·OOH: $t_{1/2}$ = 11 and 45 min, respectively). On the other hand, investigations by other groups have recently shown that these differences might be an advantage when different pathways of spin adduct formation are studied, for example, trapping of genuine hydroxyl radicals versus rearrangement of initially formed superoxide adducts.[5]

Furthermore, differentiation of carbon-centered radicals should also be possible. In view of the fact that the combined effects of the carbamoyl group[6,7] and the additional alkyl group[1–3] cannot unambiguously be predicted, we investigated a series of (methyl-) carbamoyl and alkyl substituted EMPO derivatives.

2. Results

2.1. Structure of the spin traps

All spin traps synthesized and investigated within this study can be considered as derivatives of 5-ethoxycarbonyl-5-methyl-1-pyrroline N-oxide (EMPO) in which the ethoxycarbonyl substituent has been replaced by either a $CONH_2$ or a $CONH(CH_3)$ group, and an additional methyl or ethyl group has been introduced in position 3 of the pyrroline ring. In analogy to the previously investigated compound 5-carbamoyl-5-methyl-1-pyrroline N-oxide (CAMPO[4], AMPO[6]), we suggest the following acronyms: 5-carbamoyl-3,5-dimethyl-pyrroline N-oxide (CADMPO), 3,5-dimethyl-5-methylcarbamoyl-pyrroline N-oxide (DMMCAPO), 5-carbamoyl-3-ethyl-5-methyl-pyrroline N-oxide (CAEMPO), and 3-ethyl-5-methyl-5-methylcarbamoyl-pyrroline N-oxide (EMMCAPO) (for structures, see Fig. 1a). A general synthetic scheme is given in Figure 1b.

Structural identity of the novel spin traps was confirmed by ^{13}C NMR (Table 1), ^{1}H NMR (Table 2), (HRMS analysis (Table 3), FTIR spectroscopy (Table 4) and UV–vis spectroscopy (Table 5).

A complete set of ^{1}H, H–H correlated, ^{13}C, HMQC and HMBC spectra was recorded for each compound, which allowed for a complete signal assignment in both the ^{1}H and ^{13}C domain.

Carbon NMR confirmed the presence of a heterocyclic pyrroline ring. The resonances for C-2 were found around 141–142 ppm, showing a down-field shift by about 5 ppm relative to the respective esters (approx. 136.3 ppm). Substitution caused a considerable

* Corresponding author. Tel.: +43 1 25077 4406; fax: +43 1 25077 4490.
E-mail address: Klaus.Stolze@vu-wien.ac.at (K. Stolze).

0968-0896/$ - see front matter © 2009 Elsevier Ltd. All rights reserved.
doi:10.1016/j.bmc.2009.09.006

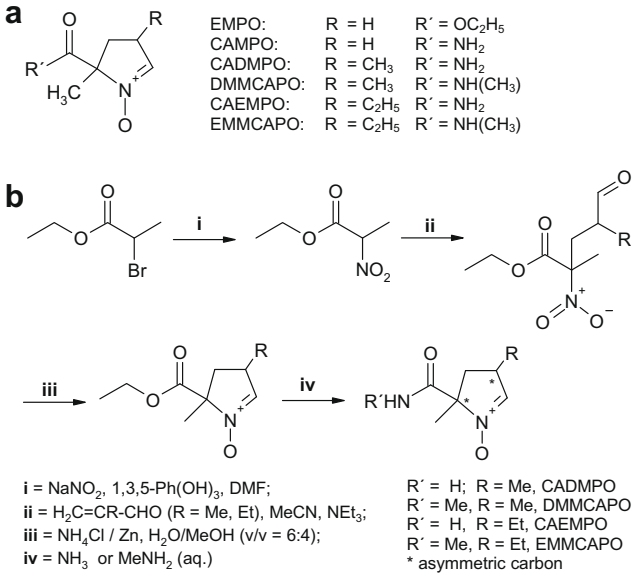

Figure 1. (a) General structure of the spin traps and (b) general synthetic scheme.

down-field shift of the C-3, resonating at 31 ppm for methyl and at 38 ppm for ethyl substituents. In non-substituted derivatives, for example, EMPO or CAMPO, the signal is found at about 25 ppm. A similar shift effect was seen for the neighboring C-4 (approx. 36–40 ppm, vs 30.6 ppm for CAMPO), and also for C-2 (141 ppm, vs approx. 135 ppm for EMPO/CAMPO).The C-5 shifts remained largely unchanged by substitution at C-3 and introduction of an amine function, being found at 78 ppm. The 5a-substituent, resonating at 20.3 ppm in EMPO, was shifted down-field by about 4 ppm, being found around 24 ppm for the derivatives described herein. The carboxylic carbon experienced a down-field shift of about 1–3 ppm (170.7–173.6 ppm) compared to the ethoxycarbonyl group of the ester counterparts (169.3–170.3 ppm). The non-substituted amides resonated at approx. 173 ppm, the *N*-methyl amides 2 ppm high-field to about 171 ppm. Due to the partial double-bond nature of the C–N bond in the amide, two atropisomers exist for the *N*-methyl derivatives, the resonances being found at 34.8/40.6 ppm in DMMCAPO and at 34.8/40.1 ppm for EMMCAPO.

The proton spectra also showed typical resonance patterns. H-2 exhibited coupling constants of around 2.8 Hz for the non-substituted amides and 2.0–2.4 Hz for the *N*-methyl amides, and appeared as a doublet. There were no shift differences between the carbamoyl derivatives (6.92–7.00 ppm) and the respective esters (about 6.97 ppm). The two amide protons were found at 5.8–6.2 ppm and at about 8.4 ppm. The significant shift difference is due to hydrogen bond formation of one amide proton to the nitrone oxygen, which is reflected in the considerable down-field shift. For the *N*-methyl amides, the above-mentioned atropisomerism is seen in the simultaneous occurrence of two resonances for the *N*-methyl group, which was found at 2.79/2.81 ppm (DMMCAPO) and 2.81/2.82 ppm (EMMCAPO), respectively. It should be noted that such comparisons are only possible if the spectra were recorded under strictly similar conditions with regard to concentration, temperature and solvent. The resonance of the 5-alkyl substituent was largely uninfluenced by the structure of the respective derivative, resonating at about 1.70 ppm. The protons at C-3a and C-4 show a strong diastereotopic splitting, which has already been noticed and discussed for the ester derivatives. The most drastic effect was seen for the C-4 methylene, where the two protons appeared as doublet of doublets at about 2.40/2.50 ppm for the *cis*-derivatives, whereas the splitting was much larger for the respective *trans*-derivatives (1.60/3.20 ppm, same splitting pattern).

The major absorption peaks in the respective FTIR spectra were seen around 1680 cm^{-1} (C=O), 1580 cm^{-1} (C=N) and 1205 cm^{-1} (N–O). The bands around 3150 cm^{-1} and 3350 cm^{-1} (N–H valence) are not always well resolved and, in addition, very sensitive to traces of humidity. They are, therefore, not listed in Table 4.

2.2. Superoxide radical adducts

Two different methods were applied in order to generate superoxide adducts: The first choice was a xanthine oxidase system which has previously been reported to be the best system for investigation of superoxide spin trapping experiments.[8,9] The results can be seen in Figure 2, where the spin traps (20 mM) were incubated in the presence of 0.2 mM hypoxanthine and 50 mU/ml xanthine oxidase (XOD) in 10 mM oxygenated phosphate buffer (pH 7.4, 1 mM DTPA). Mixtures of different spin adducts were found with CADMPO (Fig. 2a), DMMCAPO (Fig. 2b),

Table 1
^{13}C NMR data (ppm) of the spin traps

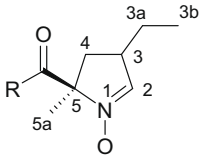

	^{2}C	^{3}C	^{3a}C	^{3b}C	^{4}C	^{5}C	^{5a}C	CO	R = $NHCH_3$
EMPO[15]	134.9	25.4	–	–	31.9	78.5	20.3	169.3	–
CAMPO[4]	135.6	25.3	–	–	30.6	79.2	22.5	174.7	–
(Lit.)[6]	137.4	25.0	–	–	30.5	79.1	24.2	172.9	–
48% *cis*-CADMPO	141.9	31.9	18.2	–	39.5	79.7	24.5	172.6	–
52% *trans*-CADMPO	141.8	32.4	18.7	–	40.9	78.6	23.9	173.6	–
47% *cis*-DMMCAPO	141.7	31.9	18.3	–	38.8	78.6	24.9	171.7	34.8/40.6
53% *trans*-DMMCAPO	141.6	32.4	18.8	–	39.7	79.6	24.1	170.7	34.8/40.6
48% *cis*-CAEMPO	140.9	38.8	26.2	11.5	36.3	78.5	24.2	173.5	–
52% *trans*-CAEMPO	140.9	39.2	26.7	11.5	37.2	79.4	24.6	172.5	–
33% *cis*-EEMCAPO	141.0	38.8	26.3	11.5	36.2	78.5	24.4	171.7	34.8/40.1
67% *trans*-EEMCAPO	141.0	39.3	26.7	11.5	37.4	79.4	24.9	170.8	34.8/40.1

Table 2
^{1}H NMR data (ppm) of the spin traps

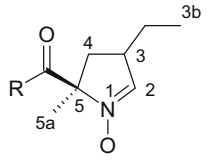

	^{2}CH	^{3}CH$_x$	^{3a}CH$_x$	^{3b}CH$_3$	^{4}CH$_2$	^{5a}CH$_3$	NH$_x$	R = NHCH$_3$	R = OC$_2$H$_5$
EMPO[15]	6.97t	2.75 m	—	—	2.16 m 2.60 m	1.72s	—	—	4.26m[a] 1.31t[b]
CAMPO[4]	6.97t	2.46–2.53 m	—	—	1.96–2.03 m 2.58–2.62 m	1.73s —	7.16s 7.38s	—	—
(Lit.)[6]	7.19t	2.79 m	—	—	2.27–2.34 m 3.14–3.20 m	1.90s —	5.85b 8.46b	—	—
48% *cis*-CADMPO	6.96d	2.94–3.03 m	1.21d	—	2.39dd 2.50dd	1.71s	6.26s 7.96s	—	—
52% *trans*-CADMPO	6.98d	2.94–3.03 m	1.18d	—	1.63dd 3.26dd	1.73s	6.26s 8.42s	—	—
47% *cis*-DMMCAPO	6.87d	2.94–3.03 m	1.20d	—	2.38dd 2.52dd	1.68s	8.56s	2.79s 2.82s	—
53% *trans*-DMMCAPO	6.92d	2.92–3.01 m	1.16d	—	1.63dd 3.26dd	1.71s	8.07s	2.78s 2.81s	—
48% *cis*-CAEMPO	6.99d	2.76–2.87 m	1.43–1.66 m	0.98q	2.33dd 2.57dd	1.72s	5.92s 8.01s	—	—
52% *trans*-CAEMPO	7.00d	2.76–2.87 m	1.43–1.66 m	0.98q	1.43–1.66 m 3.26dd	1.73s	5.92s 8.49s	—	—
33% *cis*-EMMCAPO	6.98d	2.74–2.88 m	1.42–1.68 m	0.98q	2.33dd 2.57dd	1.69s	8.58s	2.81s 2.82s	—
67% *trans*-EMMCAPO	6.96d	2.74–2.88 m	1.42–1.68 m	0.98q	1.42–1.68 m 3.28dd	1.71s	8.01s	2.80s 2.81s	—

Abbreviations: s = singlet, b = broad singlet, dd = doublet of doublets, t = triplet, m = multiplet, [a,b]from ethoxy group $^{1'}$CH$_2$ and $^{2'}$CH$_3$, respectively.

Table 3
HRMS analysis of the spin traps

	Acquired (MH)$^+$	Calcd (MH)$^+$	Error (ppm)	mDa	Acquired (MNa)$^+$	Calcd (MNa)$^+$	Error (ppm)	mDa
CAMPO	143.08543	143.0820	23.97	3.43	165.0693	165.0640	32.35	5.34
CADMPO	157.10263	157.0977	31.38	4.93	179.0870	179.0796	41.32	7.40
DMMCAPO	171.11701	171.1133	21.68	3.71	193.0103	193.0088	7.77	1.50
CAEMPO	171.11399	171.1133	4.03	0.69	207.1088	193.0952	70.43	13.6
EMMCAPO	185.15032	185.1452	27.65	5.12	207.1192	207.1108	40.55	8.40

CAEMPO (Fig. 2c), and EMMCAPO (Fig. 2d). In the case of CADMPO and CAEMPO none of the species could be attributed to a superoxide adduct. Even when XOD activity was increased to 500 mU/ml (Fig. 3a), no additional species was formed. In order to identify the individual contributions, we subtracted the spectrum recorded after 30 min (Fig. 3b) from the initial spectrum and obtained two virtually 'pure' EPR spectra. Figure 3c (corresponding to: 3c = 3a-1.85×3b) shows a species with an additional nitrogen splitting of a_N = 3.35 G and Figure 3d (corresponding to 3d = 3b-0.27×3a) an additional nitrogen splitting of a_N = 1.50 G. Simulation and superposition is shown in Figure 3e (corresponding to 23% of the species shown in Fig. 3c and 77% of the species shown in Fig. 3d). Comparison with data from the literature[10,11] and from previous studies with CAMPO[4] leads to the conclusion that the spin trap underwent oxidative degradation (Hofmann rearrangement) forming an adduct with the amino group directly attached to the pyrroline ring. As has already been mentioned in a previous paper[4] for CAMPO and its derivatives, formation of the secondary amino adduct was superoxide-dependent (no adduct formed when SOD was added prior to xanthine oxidase). Furthermore, an identical secondary species was also detected in a series of oxidizing model systems, such as hydrogen peroxide and HRP.

The suggested structure as being a 5-amino-pyrrolidine derivative is in agreement with previous studies where the DMPO amino adduct has been described by Chignell et al.[10] (a_N = 15.9 G, a_H = 19.3 G, a_N = 1.6 G) and by Kirino et al.[11] (a_N = 15.86 G, a_H = 19.04 G, a_N = 1.72 G. All data are summarized in Table 6.

While CAEMPO reacted similarly (Fig. 2c, data shown in Table 6), the respective *N*-methylamide spin traps DMMCAPO (Fig. 2b) and EMMCAPO (Fig. 2d) formed a mixture of 4 compounds, two of which were identical to the respective hydroxyl radical adduct, as can be seen in Figure 4 for the DMMCAPO/HX/XOD system, recorded both immediately after mixing (Fig. 4a) and after 30 min (Fig. 4b). Spectral subtraction shown in Figure 4c (corresponding to 4c = 4a-0.39×4b) lead to one isomer of the superoxide adducts (a_N = 13.34 G, a_H = 14.55 G). The second difference spectrum shown in Figure 4d (corresponding to 4d = 4b-1.20×4a) still consisted of several species. However, subsequent subtraction of adequate contributions of the hydroxyl radical adduct (see below, Fig. 6b) led to the practically pure spectrum shown in Figure 4e, the second isomer of superoxide adducts (a_N = 13.20 G, a_H = 6.20 G). The same procedure was done with the spectrum of EMMCAPO (Fig. 2d, data listed in Table 6). Formation of Hofmann rearrangement products was not observed (no second nitrogen splittings visible).

Table 4
IR data (cm^{-1}) of the spin traps

EMPO[15]	**2985**	**2940**	2874	**1741**	–	**1582**	**1464**	**1446**	**1377**	1341	**1288**	**1236**	**1182**	**1107**	–	**1024**	–	950	926	**862**	796	–	–	–	–
CAMPO	**3047**	2939	2784	**1679**	1630	**1587**	1475	**1446**	**1396**	1379	**1298**	**1218**	**1199**	1115	1097	1029	998	953	885	843	744	700	**656**	–	**611**
CADMPO	**2970**	**2913**	2875	**1688**	**1628**	**1576**	**1447**	–	**1386**	–	–	**1214**	–	**1110**	–	–	966	939	–	812	752	720		**634**	–
DMMCAPO	**2965**	**2935**	2876	**1673**	–	**1552**	**1455**	1411	1377	1298	–	**1221**	–	1109	–	–	965	934	–	830	782	–		634	–
CAEMPO	**2964**	**2934**	**2876**	**1691**	**1645**	**1572**	**1457**	–	**1391**	**1365**	–	**1218**	**1189**	**1114**	–	1021	–	932	–	–	790	–		**635**	–
EMMCAPO	**2963**	**2927**	**2876**	**1693**	–	**1552**	**1458**	**1411**	1381	1292	–	**1222**	1143	1114	–	1021	–	935	883	–	783	–	669	–	**594**

Intensities: **strong** (**1741**), **medium** (**1464**), weak (950).

Table 5
Half-life of the superoxide adducts, *n*-octanol/buffer partition coefficients, and UV–vis spectroscopic data of the spin traps

Compound	Apparent $t_{1/2}$ (min)		Partition coefficient *n*-octanol/phosphate buffer (100 mM, pH 7.0)	UV data λ_{max} and molar absorptivity ϵ ($l\ mol^{-1}\ cm^{-1}$)
EMPO[14,15]	8.6		0.15	231 nm, 7417
CAMPO[4,6]	8.58		0.016	232 nm, 7652
CADMPO	–	(14.5*)	0.049	232 nm, 8732
DMMCAPO	11.2	(10.1*)	0.068	232 nm, 8858
CAEMPO	–	(17.4*)	0.143	232 nm, 8026
EMMCAPO	36.6**	(19.8*)	0.216	232 nm, 8522

*KO_2 system, **Sum of ·OOH and ·OH signals.

We also tested a second superoxide-generating system, consisting of an aqueous solution of CADMPO (40 mM), to which a small amount of solid KO_2 (approx. 0.5 mg) was added. Immediately thereafter the solution was neutralized by 1:1 dilution with 300 mM phosphate buffer pH 7.0, containing 20 mM DTPA, SOD (250 U/ml) and catalase (250 U/ml), giving a final pH of about 7.4. After that, the ESR spectrum was recorded (Fig. 5 a), showing broadened lines due to the participation of several diastereomeric forms. Computer simulation gave a best fit assuming three distinct isomeric forms (a_N = 13.03 G, a_H = 8.35 G, 39%; a_N = 13.18 G, a_H = 4.72 G, 31% a_N = 13.16 G, a_H = 6.24 G, 30%), one of them being very similar to the second isomer found in the XOD system (Fig. 5e). However, unequivocal identification does not seem to be possible due to the high line width. Similar spectra were obtained from DMMCAPO (Fig. 5b), CAEMPO (Fig. 5c), and EMMCAPO (Fig. 5c), their HFS parameters being listed in Table 6.

Decay kinetics of the superoxide adducts were calculated as follows: A series of repetitive scans was recorded for each incubation (every 90 s for 30 min) using a first-order exponential decay approximation (Table 5, Pearson correlation coefficient R^2 >0.96). As shown in Figures 4 and 5, the presence of different isomers and secondary products strongly interfered. Therefore, kinetic calculations of the half lives of the respective superoxide adducts can only be regarded as approximations.

2.3. Hydroxyl radical adducts

When the spin traps (40 mM) were incubated for 10 s in the presence of a previously described aqueous Fenton system,[4,12] consisting of hydrogen peroxide (0.2%), EDTA (2 mM), and iron-(II) sulfate (1 mM) and the reaction was stopped upon 1:1 dilution with phosphate buffer (300 mM, pH 7.4) containing DTPA (20 mM), the respective hydroxyl radical adducts were obtained (Fig. 6). Computer simulations of the obtained spectra are only approximations, the distorted line form suggests participation of unresolved stereoisomers due to three asymmetric carbon atoms in the spin adducts. In principle, two different isomers were found for CADMPO/·OH (ratio 62/38; Fig. 6a, variable contribution of Hofmann degradation products is also observed) DMMCAPO/·OH (ratio 53/47; Fig. 6b) and EMMCAPO/·OH (ratio 77/23; Fig. 6d), and three for CAEMPO/·OH (ratio 53/30/17; Fig. 6c).

2.4. Strong dependence of EPR spectra on the spin trap as well as the size of trapped carbon-centered radicals

We first tested the influence of the different spin traps while using a methyl radical generating Fenton system,[4,12] consisting of the respective spin trap (40 mM), hydrogen peroxide (0.2%),

EDTA (2 mM), and iron-(II) sulfate (1 mM) in a mixture of DMSO with water (20/80, v/v). After 10 s, the reaction was stopped upon 1:1 dilution with phosphate buffer (300 mM, pH 7.4) containing DTPA (20 mM). The results can be seen in Figure 7. While two diastereomeric forms were detected from the amides CADMPO/·CH_3 (Fig. 7a; a_N = 15.38 G, a_H = 15.38 G, 55%; and a_N = 15.31 G, a_H = 22.20 G, 45%), and CAEMPO/·CH_3 (Fig. 7c; a_N = 15.10 G, a_H = 14.94 G, 53%; and a_N = 15.41 G, a_H = 25.50 G, 47%), only one isomer was formed from the methylamides, DMMCAPO/·CH_3 (Fig. 7b, a_N = 15.04 G, a_H = 15.36 G), and EMMCAPO/·CH_3 (Fig. 7d, a_N = 15.06 G, a_H = 14.39 G). The latter two compounds are therefore better suited for methyl radical trapping due to the characteristic feature of the obtained ESR spectra.

In a second step the spin trap DMMCAPO was used throughout all experiments while the compound added for generating the carbon-centered radical was varied: DMSO (20%), methanol (20%), ethanol (20%) or sodium formate (200 mM) were added to the Fenton-type incubation system[4,12] mentioned above in Figure 7, incubated for 10 sec and 1:1 diluted with phosphate buffer (300 mM, pH 7.4) containing DTPA (20 mM). The results can be seen in Figure 7a to d (for the methyl, hydroxymethyl, hydroxyethyl and carbon dioxide anion radical, respectively). The ratio of the two predominant diastereomeric forms varied considerably, the methyl radical adduct being predominantly the isomer with low hydrogen HFS (Fig. 7a) whereas the larger hydroxyethyl radical preferably formed the isomer having a larger hydrogen HFS (Fig. 7c). We also performed spin trapping experiments using ^{13}C labeled methanol (spectrum not shown, data listed in Table 6). A larger hydrogen HFS always corresponded to a lower carbon HFS, indicating a more equatorial arrangement of the residue, and vice versa, corresponding to a more axial structure. In addition, impurities stemming from "OH adducts' showed less interference due to the absent extra splitting. In these cases estimation of the relative stabilities of the two isomeric forms was possible. The more equatorial form was considerably less stable (strong deviation from first-order, but 'half-life' around 5–8 min), whereas the more axial form was

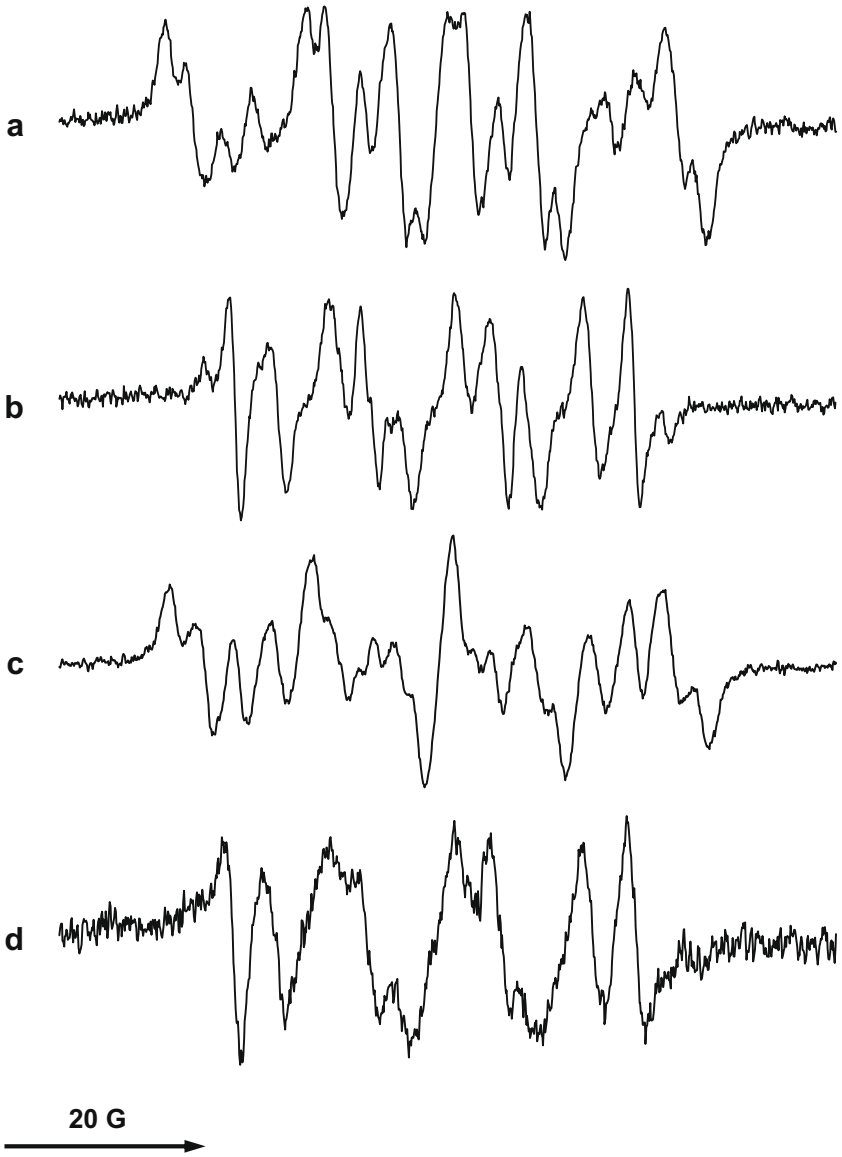

Figure 2. Mixture of radicals formed from the spin traps CADMPO, DMMCAPO, CAEMPO, and EMMCAPO incubated with hypoxanthine/xanthine oxidase. (a) CADMPO (20 mM), hypoxanthine (0.2 mM) and xanthine oxidase (50 mU/ml) in oxygenated phosphate buffer (10 mM, pH 7.4, containing 1 mM DTPA) were measured immediately after mixing using the following EPR parameters: sweep width, 80 G; modulation amplitude, 0.52 G; microwave power, 20 mW; time constant, 0.08 s; receiver gain, 5×10^4; scan rate, 57 G/min. (b) same as in (a), except that DMMCAPO was used. (c) Same as in (a), except that CAEMPO was used. (d) Same as in (a), except that EMMCAPO was used.

quite stable ('half-life' >40 min). The large differences in both, HFS parameters and stabilities might therefore be useful for unequivocal identification of the specific carbon-centered radical trapped. The respective HFS data are listed in Table 6.

2.5. Additional radical adducts formed

In addition to the superoxide, hydroxyl, methyl, hydromethyl, hydroxyethyl and carbon dioxide anion radical adducts shown in Figs. 2–8 we also tried to detect the respective methoxyl radical adducts using the method previously described by Dikalov et al.[13]which had been successfully applied in our previous studies.[1–4] Unfortunately we were only able to detect the respective $^{\cdot}OCH_3$ adducts with DMMCAPO and EMMCAPO (see Table 6). With CADMPO and CAEMPO only hydroxymethyl adducts and Hofmann rearrangement products were detected (not shown).

We also investigated the formation of reduction products of the spin traps ($H^{\cdot}$ adducts). For this purpose, a small amount of KBH_4

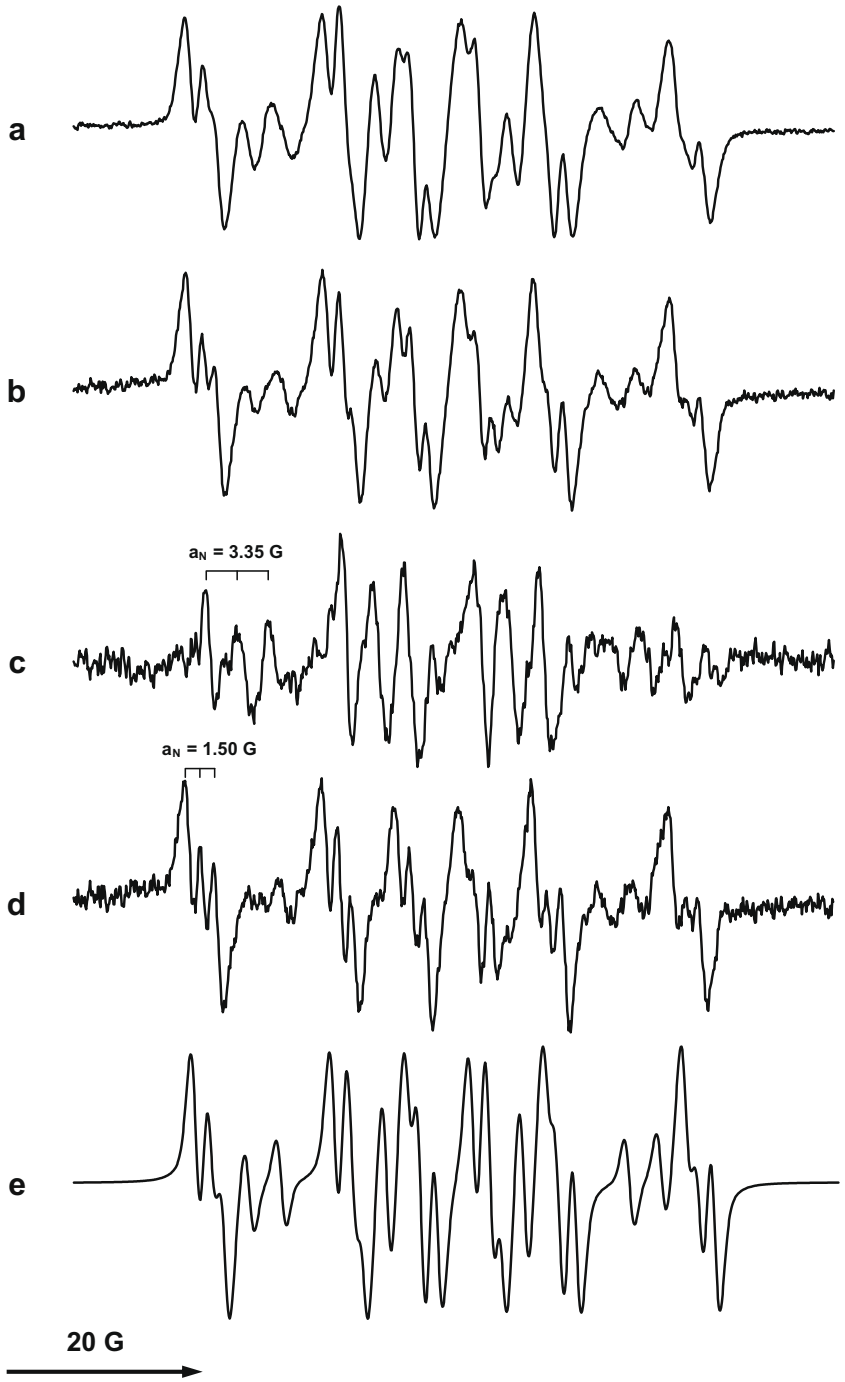

Figure 3. Mixture of radicals formed from the spin trap CADMPO incubated with hypoxanthine/xanthine oxidase. (a) CADMPO (20 mM), catalase (250 U/ml), hypoxanthine (0.2 mM) and xanthine oxidase (500 mU/ml) in oxygenated phosphate buffer (20 mM, pH 7.4, containing 0.4 mM DTPA) were measured immediately after mixing using the following EPR parameters: sweep width, 80 G; modulation amplitude, 0.52 G; microwave power, 20 mW; time constant, 0.08 s; receiver gain, 5×10^4; scan rate, 57 G/min. (b) spectrum recorded after 30 min. (c) difference (3a-1.85×3b), showing one of the isomers of Hofmann rearrangement. (d) Difference (3b-0.27×3a), showing the second isomer of Hofmann degradation. (e), computer simulation of the spectrum shown in Figure 4a, assuming the contribution of 23% of isomer 1 and 77% of isomer 2 of the Hofmann degradation products (see Table 6 for details).

Table 6
Comparison of the EPR parameters of different radical adducts of various EMPO amino derivatives

Radical	HFS (G)	EMPO[4,14]			CAMPO		CADMPO			DMMCAPO			CAEMPO			EMMCAPO		
XOD system		*Trans*[4]		*Cis*[4]														
(·OOH)		(94%)[x]		(6%)	(80%)[5]	(20%)[5]	–		–	(64%)		(36%)	–		–	(80%)	(20%)	
	a_N	13.27	13.25	13.25	13.0	13.1	–		–	13.20		13.34	–		–	12.90	13.45	
	a_H	12.37	9.30	10.15	10.8	12.5	–		–	6.20		14.55	–		–	7.25	14.55	
	a_H	(55.5%/44.5% of *trans*[x])		1.50	–	1.75	–		–	–		–				1.20	–	
('Hofmann')			–		(100%)*		(77%)		(23%)*	–	–	–	–	(53%)		(47%)*	–	–	–
	a_N		–		14.43		14.51		14.38	–	–	–	–	14.08		14.55	–	–	–
	a_H		–		19.34		22.24		14.38	–	–	–	–	12.40		21.94	–	–	–
	a_N		–		2.17		1.50		3.35	–	–	–	–	3.75		1.70	–	–	–
	a_H		–		–		–		–	–	–	–	–	0.70		–	–	–	–
KO_2 system:		–		–	(50%)	(50%)	(39%)	(31%)	(30%)	(63%)	(19%)	(18%)		(68%)	(21%)	(11%)	(52%)	(24%)	(24%)
	a_N	–		–	13.19	13.19	13.03	13.18	13.16	13.23	13.12	13.07		13.16	13.14	13.13	13.31	13.07	13.07
	a_H	–		–	9.89	12.09	8.35	4.72	6.24	5.65	6.08	8.60		5.11	5.50	8.75	5.00	8.60	6.18
		Trans[4]		*Cis*[4]															
·OH		(76%)		(24%)	(81%)	(19%)	(62%)		(38%)#	(53%)		(47%)		(53%)	(30%)	(17%)#	(77%)	(23%)	
	a_N	14.11		14.18	13.97	13.95	13.72		14.51	13.78		14.28		13.78	14.34	14.48	13.73	14.38	
	a_H	12.80		15.27	13.64	12.45	9.00		18.84	9.05		18.70		8.45	18.07	18.90	7.95	18.24	
	a_H	0.63		0.62	–	–	–		–	–		–		0.90					
	a_H	0.43		0.50	(69%)[5]	(31%)[5]	–		–	–		–		0.75					
	a_H	0.21(3)		0.29(3)	a_N	14.0	14.0												
	a_H	0.13(2)		0.07(2)	a_H	13.5	12.5												

Radical	HFS (G)	EMPO[14]		CAMPO		CADMPO			DMMCAPO			CAEMPO			EMMCAPO		
H		(100%)		(100%)		(51%)		(49%)	(55%)		(45%)	(66%)		(34%)	(59%)		(41%)
	a_N	15.52		15.30		15.35		15.14	15.35		15.18	15.38		14.99	15.35		15.18
	a_H	22.21		22.23		24.67		26.00	24.35		25.89	24.97		26.20	24.99		26.09
	a_H	20.82		20.00		17.28		16.10	17.28		16.14	17.05		16.40	17.08		16.32
·CH_3		(100%)		(100%)		(55%)		(45%)	(100%)			(53%)		(47%)	(100%)		
	a_N	15.42		15.15		15.38		15.31	15.04			15.10		15.41	15.06		
	a_H	22.30		21.43		15.38		22.20	15.36			14.94		25.50	14.39		
	a_H	–		–		–		–	–			–		–	–		
·OCH_3		(50%)	(50%)	(74%)	(26%)		–		(100%)			–			(100%)		
	a_N	13.74	13.74	14.37	14.63		–		13.57			–			13.45		
	a_H	10.87	7.81	19.14	19.81		–		5.91			–			5.35		
	a_H	–	–	2.13	–		–		–			–			–		
·CH_2OH		(100%)		(100%)		(71%)		(30%)	(63%)		(37%)	(70%)	(30%)		(51%)		(49%)
	a_N	14.95		14.75		14.80		14.64	14.85		14.62	14.81	14.57		14.86		14.56
	a_H	21.25		21.20		24.54		16.43	24.48		16.68	23.90	15.76		23.87		15.86
	a^{13C}	–		–		6.10		9.53	6.08		9.56	6.52	9.95		6.49		9.88
·$CH(OH)CH_3$		(67%)	(33%)	(100%)		(84%)		(16%)	(81%)		(19%)	(93%)	(7%)		(79%)		(21%)
	a_N	14.94	15.00	14.77		14.75		14.80	14.66		14.60	14.71	14.60		14.63		14.45
	a_H	20.82	22.40	21.34		23.00		16.64	23.02		16.50	21.90	16.50		21.65		15.80
·CO_2^-		(100%)		(58/53[5] %)	(42/47[5] %)		(49%)	(41%)	(10%)	(51%)	(49%)	(41%)	(41%)	(18%)	(63%)		(37%)
	a_N	14.74		14.46/14.53[5]	14.20/14.25[5]		14.60	14.40	13.80	14.45	14.50	14.55	14.50	14.20	14.45		14.00
	a_H	17.16		16.62/16.48[5]	18.30/18.15[5]		21.57	14.40	22.86	14.45	21.32	21.30	13.85	23.14	14.45		22.66
	a_H	–	–	–	–	–	–	0.40(4)	–	0.40(4)	–	–	0.38(4)	–	–	–	

[4,5,14]: data from Culcasi et al.,[4] Villamena et al.,[5] Stolze et al.,[14] [x] mixture of rotamers, [*] variable contribution of HO· adduct*, [#]variable contribution of Hofmann product#.

(ca. 0.5 mg/500 μl) was added to an aqueous spin trap solution (40 mM), incubated for 1 min, after which the pH was readjusted to pH 7.4 by 1:1 dilution with phosphate buffer (300 mM, pH 7.4, containing 20 mM DTPA). An overview of all ESR-spectral parameters is given in Table 6.

3. Discussion

Four novel carbamoyl or methylcarbamoyl derivatives of the spin trap EMPO were synthesized in this study and compared with the previously obtained spin trap CAMPO[4] (AMPO[6,7]) and its derivatives. The chemical structure and purity of all compounds was comprehensively supported by full NMR assignment (^{1}H and ^{13}C), ESI Q-TOF MS, FTIR, and UV–vis spectroscopy (Tables 1–5).

Our findings showed that a variety of products were formed in superoxide-generating systems, especially when hypoxanthine/xanthine oxidase was used. Although the observed half lives of the superoxide adducts are within the range of suitable spin traps, such as EMPO[8,14–18] or DEPMPO,[19] the formation of isomers and secondary products does not render these compounds appropriate

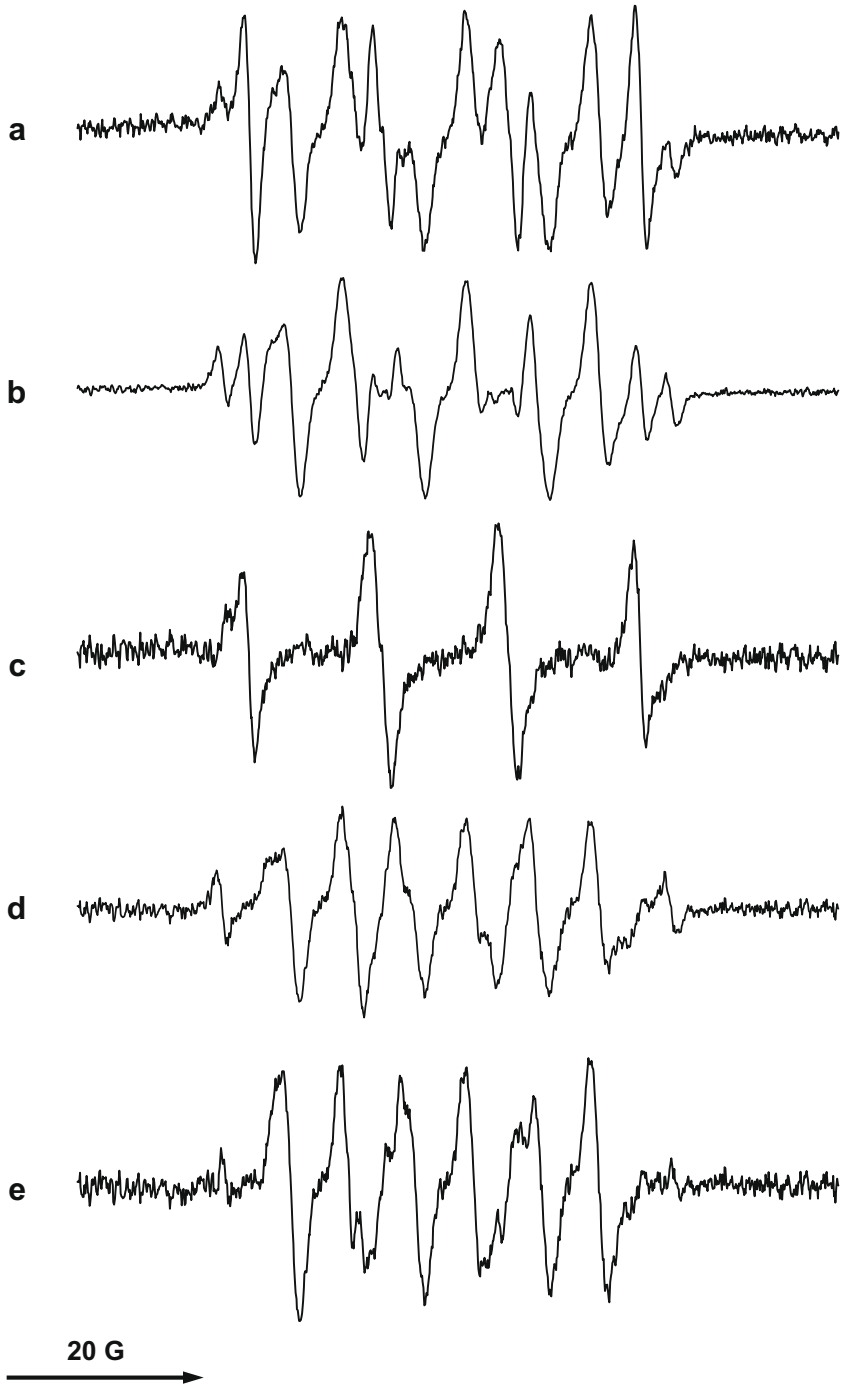

Figure 4. Mixture of superoxide and hydroxyl radical adducts formed from DMMCAPO incubated with hypoxanthine/xanthine oxidase. (a) DMMCAPO (20 mM), catalase (250 U/ml), hypoxanthine (0.2 mM) and xanthine oxidase (50 mU/ml) in oxygenated phosphate buffer (10 mM, pH 7.4, containing 1 mM DTPA) were measured immediately after mixing using the following EPR parameters: sweep width, 80 G; modulation amplitude, 0.52 G; microwave power, 20 mW; time constant, 0.08 s; receiver gain, 5×10^4; scan rate, 57 G/min. (b) Spectrum recorded after 30 min. (c) Difference (Fig. 4a-0.39×Fig. 4b), (d) difference (Fig. 4b-1.20×Fig. 4a), (e) difference (Fig. 4d-1.80×Fig. 6b, that is, elimination of impurities stemming from the ·OH adduct, (see Table 6 for details).

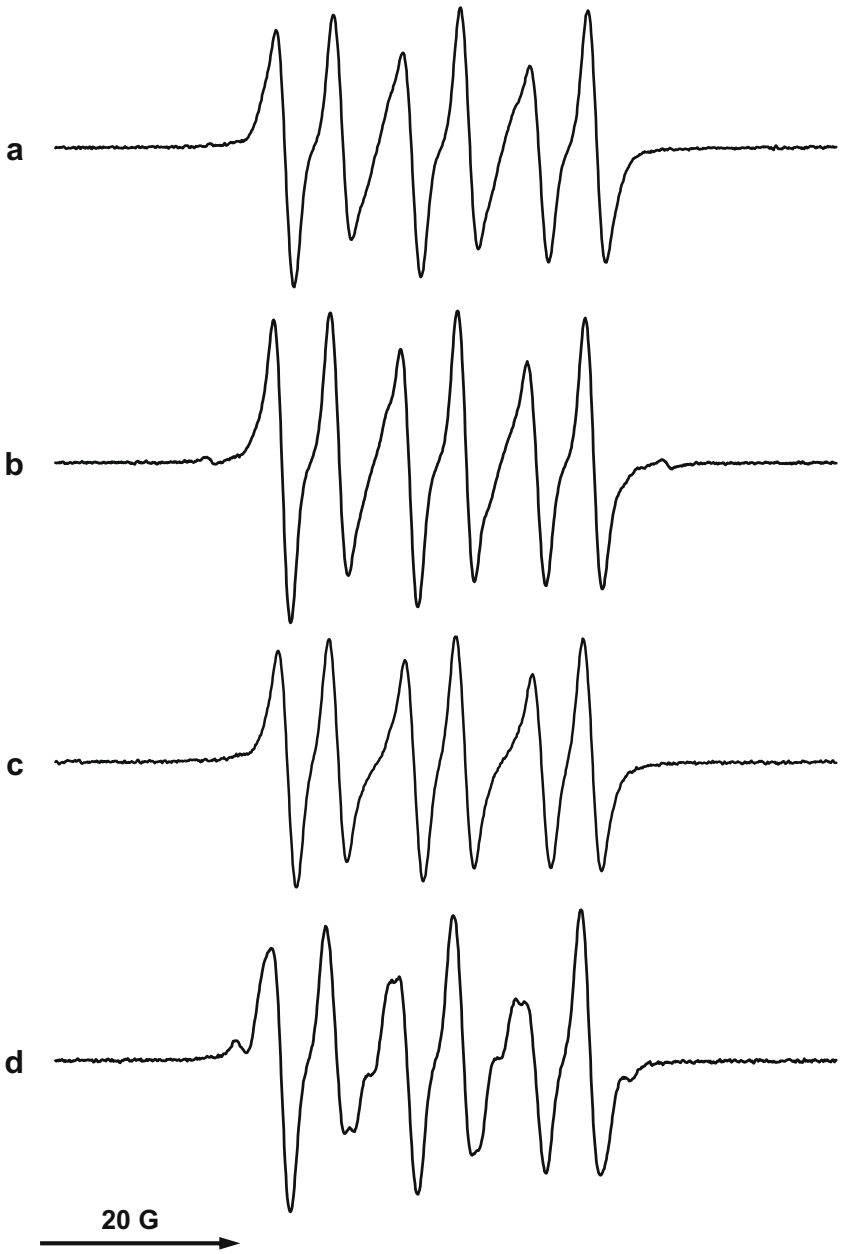

Figure 5. Measurement of superoxide radical spin adducts formed from CADMPO, DMMCAPO, CAEMPO, and EMMCAPO and solid KO_2. (a) CADMPO (40 mM) was dissolved in 250 μl water, a small amount of solid KO_2 (approx. 0.5–1 mg) was added and the solution was immediately neutralized thereafter by 1:1 dilution using 300 mM phosphate buffer pH 7.0, containing 20 mM DTPA, SOD (250 U/ml) and catalase (250 U/ml), giving a final pH of about 7.4. The spectrum was recorded immediately thereafter (Fig. 2a) using the following EPR parameters: sweep width, 80 G; modulation amplitude, 0.10 G; microwave power, 20 mW; time constant, 0.08 s; receiver gain, 2.5×10^4; scan rate, 57 G/min. (b) Same as in (a), except that DMMCAPO was used. (c) Same as in (a), except that CAEMPO was used. (d) Same as in (a), except that EMMCAPO was used.

for unequivocal detection of superoxide, especially in biological systems where additional adduct species can be formed from a variety of substances present. We therefore did not explore the superoxide trapping in more detail and did not determine the individual rate constants of the superoxide trapping reactions. They were just roughly estimated to be similar or even smaller compared to EMPO or DEPMPO. A further drawback when using carbamoyl derivatives (CADMPO and CAEMPO) is significant formation of Hofmann rearrangement products under oxidizing conditions. This reaction (though not observed in the presence of SOD) is not specific for superoxide. It is also observed in Fenton-type systems, using hydrogen peroxide/HRP incubations, or especially in hypohalite solutions.[4]

Hydroxyl radical detection is especially difficult with CADMPO (and, to a minor extent, with CAEMPO) due to the presence of Hofmann degradation products, which are absent while using the methylcarbamoyl compounds DMMCAPO or EMMCAPO.

Methoxyl radical adducts were rather unstable and were rapidly replaced by the respective carbon-centered hydroxymethyl adducts, which were considerably more stable.

On the other hand, the novel compounds seem to be predisposed for the detection of carbon-centered radicals, and they are valuable tools for the distinction between small carbon-centered radicals, such as methyl, hydroxymethyl, hydroxyethyl or carbon dioxide anion radicals, as the ratio of the two major diastereomeric forms strongly depends on the size of the trapped radical (see Fig. 8).

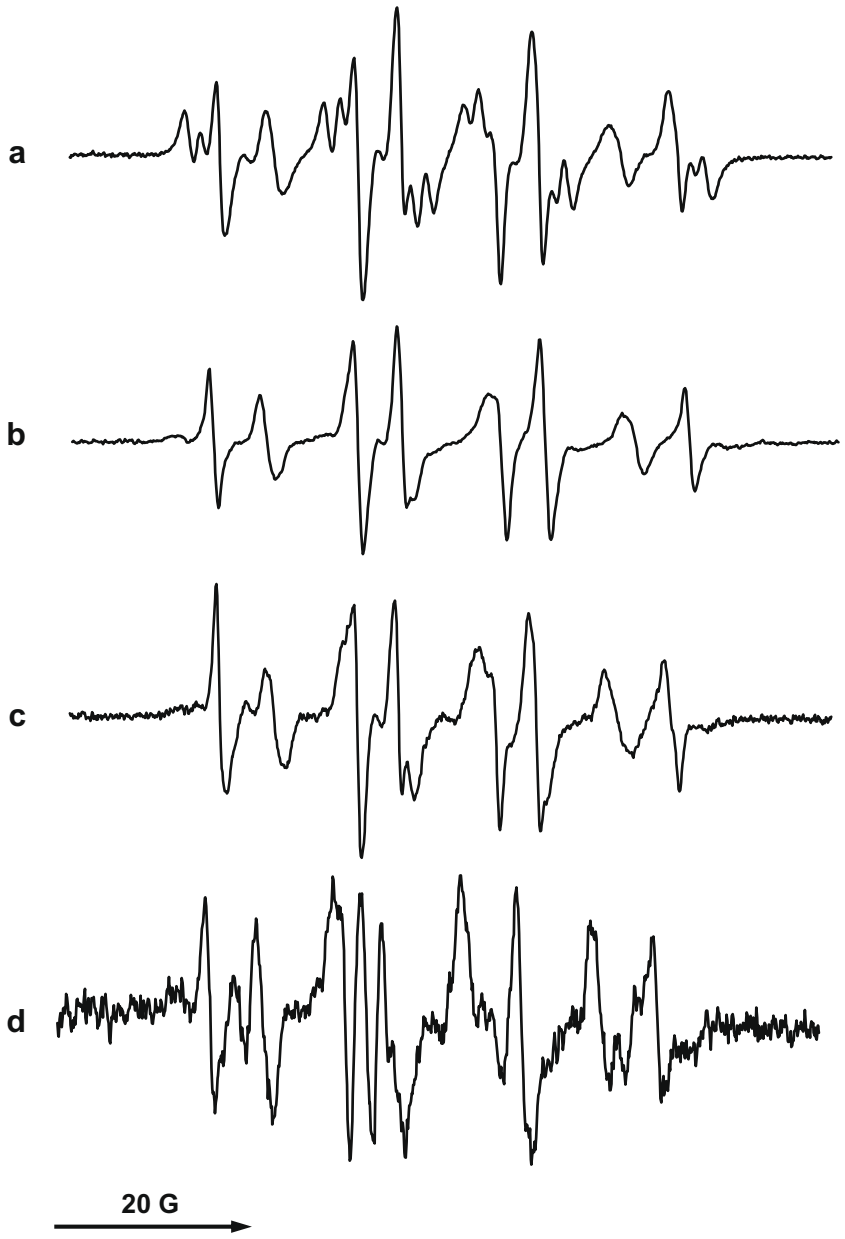

Figure 6. Iron-dependent formation of hydroxyl radical spin adducts from CADMPO, DMMCAPO, CAEMPO, and EMMCAPO. (a) CADMPO (40 mM, initial concentration) was incubated with a Fenton system containing $FeSO_4$ (1 mM), EDTA (2 mM), H_2O_2 (0.2%). The reaction was stopped after 10 s by 1:1 dilution with phosphate buffer (300 mM, pH 7.4, containing 20 mM DTPA) and the spectrum was recorded using the following spectrometer settings: sweep width, 80 G; modulation amplitude, 0.21 G; microwave power, 20 mW; time constant, 0.08 s; receiver gain, 5×10^4; scan rate, 57 G/min. (b) Same as in (a), except that DMMCAPO was used. (c) Same as in (a), except that CAEMPO was used. (d) Same as in (a), except that EMMCAPO was used.

4. Conclusion

In conclusion, though all four novel EMPO-derived carbamoyl or methyl carbamoyl derivatives formed superoxide adducts of similar or even higher stability compared to EMPO[8,14–18] itself and sometimes equal to DEPMPO[19], they cannot be recommended for superoxide trapping. Low spectral intensity, the presence of several diastereomeric isomers and formation of secondary products (hydroxyl radical adducts and Hofmann degradation products) leads to very complicated spectra.

However, the formation of only two different diastereomeric forms from DMMCAPO and EMMCAPO is an advantage when carbon-centered radicals are trapped. The characteristic ratio between these forms allows distinction between methyl, hydroxymethyl, hydroxyethyl and carbon dioxide anion radical adducts.

5. Experimental

5.1. Chemicals

Ethacrolein, methacrolein and triethylamine were commercially available from Fluka, all other chemicals were obtained from VWR.

5.2. Syntheses

Synthesis and characterization of the compounds were performed in analogy to those reported previously[1–3] for the synthesis of derivatives of EMPO[14–18] and CAMPO[4,6,7] with minor adaptations as given below.

5.2.1. Synthesis of ethyl 2-nitropropionate

Ethyl 2-bromopropionate (10.9 g, 60 mmol) was added under stirring to a solution of sodium nitrite (7.2 g, 104 mmol) and phloroglucinol (6.6 g, 52 mmol) in dry *N,N*-dimethylformamide (120 ml) at room temperature. The solution was stirred overnight, poured into ice water (240 ml), and extracted four times with ethyl acetate (100 ml). The combined extracts were treated with 100 ml of a $NaHCO_3/Na_2CO_3$ solution and dried over $MgSO_4$. After removal of the solids by filtration, the solvent was evaporated in vacuo. Deeply colored products were extracted with water. After removal of the solvent from the organic phase, the pale yellow product was used without further purification, the aqueous phase (containing the major part of the colored impurities) was discarded. Average yield: 85% (crude product).

5.2.2. Ethyl 2-methyl-2-nitro-4-formylalkanoate

Ethyl 2-nitropropionate (3.4 g, 23 mmol) was dissolved in a mixture of acetonitrile (10 g, 244 mmol) and triethylamine (0.2 g, 2 mmol). Methacrolein (2.7 g, 38 mmol, for CADMPO and DMMCAPO) or ethacrolein (3.2 g, 38 mmol, for CAEMPO and EMMCAPO) was slowly added at 0 °C. The solution was kept at 10 °C for 1.5 h and then poured into a solution of ice-cold HCl (5 ml of concentrated HCl in 150 ml of water). The solution was extracted 3 times with CH_2Cl_2 and dried over $MgSO_4$. After filtration, the mixture was

Figure 7. Comparison of iron-dependent formation of methyl radical spin adducts from the spin traps CADMPO, DMMCAPO, CAEMPO, and EMMCAPO. (a) A Fenton system was used with the following initial concentrations: CADMPO (40 mM), $FeSO_4$ (1 mM), EDTA (2 mM), H_2O_2 (0.2%) in 20% aqueous DMSO. The reaction was stopped after 10 s by 1:1 dilution with phosphate buffer (300 mM, pH 7.4, containing 20 mM DTPA) and the spectrum was recorded using the following spectrometer settings: sweep width, 80 G; modulation amplitude, 0.21 G; microwave power, 20 mW; time constant, 0.08 s; receiver gain, 5×10^4; scan rate, 57 G/min. (b) Same as in (a), except that DMMCAPO was used. (c) Same as in (a), except that CAEMPO was used. (d) Same as in (a), except that EMMCAPO was used.

distilled under reduced pressure, and the purity of the remaining product was assessed by thin layer chromatography and IR spectroscopy. Average yield: 84% (crude product).

5.2.3. Synthesis of the nitrones

Synthesis of the nitrones was performed according to the procedure described recently for the synthesis of CAMPO derivatives.[4] To a concentrated solution of 25 mmol of the respective ethyl-2-methyl-2-nitro-4-formylalkanoate in H_2O/CH_3OH (v/v = 6:4) an aqueous solution of ammonium chloride (1.87 g in 8 ml of water) was added. While zinc dust (8.5 g, 130 mmol) was slowly added within 30 min, the mixture was carefully kept at room temperature. The mixture was stirred for 4.5 h at room temperature, the white precipitate and the remaining zinc powder were removed by filtration, and the residue was washed five times with methanol (30 ml). The liquid phase was concentrated to about 10 ml and extracted four times with 60 ml CH_2Cl_2. The organic phase was dried with $MgSO_4$, filtered and concentrated. Column chromatography on silica gel with a petroleum ether/ethanol gradient allowed the separation from the majority of side products and provided a dark yellow or light brown product. Additional purification was done on a 1 ml solid phase extraction column using a Chromabond C-18 100 mg column obtained from Macherey-Nagel (Düren, Germany) using a water/methanol gradient as the eluant. Colored solutions were subjected to the same procedure until the solution containing the N-oxides remained colorless. The products were extracted

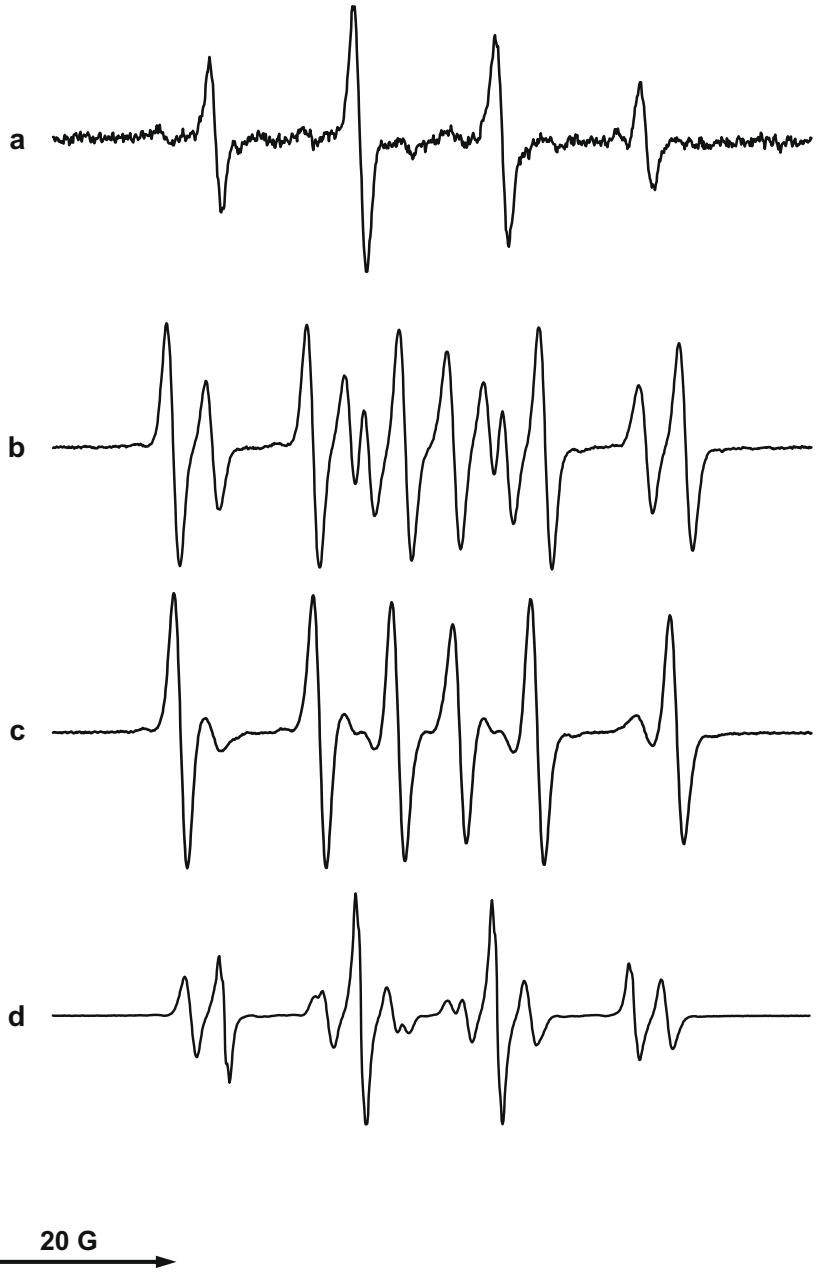

Figure 8. Comparison of different carbon-centered radical spin adducts from DMMCAPO, generated in a Fenton system in the presence of DMSO, methanol, ethanol or formate. (a) A Fenton system was used with the following initial concentrations: DMMCAPO (40 mM), $FeSO_4$ (1 mM), EDTA (2 mM), H_2O_2 (0.2%) in 20% aqueous DMSO. The reaction was stopped after 10 s by 1:1 dilution with phosphate buffer (300 mM, pH 7.4, containing 20 mM DTPA) and the spectrum was recorded using the following spectrometer settings: sweep width, 80 G; modulation amplitude, 0.21 G; microwave power, 20 mW; time constant, 0.08 s; receiver gain, 5×10^4; scan rate, 57 G/min. (b) same as in (a), except that DMSO was replaced by methanol. (c) Same as in (a), except that ethanol was used. (d) Same as in (a), except that sodium formate (200 mM) was used.

three times with CH_2Cl_2, the solvent was removed and the identity checked by TLC, IR and UV–vis spectroscopy. Average yield: 40–50% (purified product).

5.2.4. Synthesis of the 3,5-dialkyl-5-carbamoyl and 3,5-dialkyl-5-methylcarbamoyl pyrroline N-oxides

Synthesis of the 3,5-dialkyl-5-carbamoyl- or 5-methylcarbamoyl pyrroline N-oxides was performed in analogy to CAMPO (AMPO) according to Villamena et al.[6,7] Briefly, the respective nitrones (3,5-EDPO or 3,5-EEMPO) were dissolved in aqueous ammonia solution (for the 3,5-dialkyl-5-carbamoyl compounds) or methylamine solution (for the 3,5,dialkyl-5-methylcarbamoyl compounds) and stirred for several days until the spot (TLC) or peak (HPLC) of the original N-oxide had completely disappeared or larger amounts of secondary products were formed. After removal of the aqueous ammonia solution (or methylamine solution, respectively), the crude products were subjected to column chromatography on silica gel using methylene chloride/ethanol mixtures as the eluants. After purification on 1 ml solid phase extraction columns as described above (Chromabond C-18 100 mg columns), the compounds were obtained as white crystals or colorless oils that crystallized in the refrigerator after several days. The purity of the obtained products was assessed by TLC, HPLC, and UV–vis spectroscopy. Final identification of the purified products was performed by ^{1}H NMR, ^{13}C NMR, and IR spectroscopy. Purity was confirmed by HRMS (see Table 3). Average yield: 20–30% (purified product). An attempt to synthesize the respective dimethylcarbamoyl compounds using aqueous dimethylamine under otherwise identical conditions failed. Instead, a variety of dark colored products was formed, among which only the dimethylammonium salt of the respective carboxylic acid (ca. 10–20%) could be identified. Isolation and purification was not possible.

5.3. Instruments

NMR spectra were recorded on a Bruker Avance at 400 MHz for ^{1}H, and 100 MHz for ^{13}C at 22 °C. $CDCl_3$ was used as the solvent throughout, TMS (tetramethylsilane) as the internal standard. Concentrations were set to 10 mg sample/0.6 ml solvent, temperature to 293 K. ^{13}C peaks were assigned by means of APT (attached proton test), HMQC (^{1}H-detected heteronuclear multiple-quantum coherence) and HMBC (heteronuclear multiple bond connectivity) spectra. All chemical shift data are given in ppm units (Tables 1 and 2). Mass spectra were obtained as follows (Table 3). Samples were diluted in the ratio 1:10,000 in 70% methanol containing 0.1% formic acid and injected offline to ESI Q-TOF MS on a Waters Micromass Q-TOF Ultima Global. IR spectra were recorded as film on an ATI Mattson Genesis Series FTIR spectrometer (see also Table 4). UV–vis spectra were recorded on Hitachi 150-20 and U-3300 spectrophotometers in double-beam mode against a blank of the respective solvent (Table 5). Determination of the concentrations was done measuring the absorption maxima in the range between 200 and 300 nm. For determination of the partition coefficients, 500 μl of *n*-octanol was added to 500 μl of a solution of the respective spin trap (100 mM or 5–10 mg, respectively) in 100 mM phosphate buffer, pH 7.4. The mixture was vortexed for 2 min at room temperature. If necessary, the procedure was repeated several times, until an equilibrium between the two phases was achieved. After careful separation of the phases, the absorbance was read at the maximum around 235 nm after dilution with methanol. For EPR experiments, Bruker spectrometers (ESP300E and EMX) were used, operating at 9.7 GHz with 100 kHz modulation frequency, equipped with a rectangular TE_{102} or a TM_{110} microwave cavity. All calculations for spectral simulation were done using the SimFonia Program by Bruker (Table 6).

Acknowledgments

The authors wish to thank P. Jodl for skillful technical assistance in synthesis, purification, and characterization of the spin traps.

References and notes

1. Stolze, K.; Rohr-Udilova, N.; Rosenau, T.; Stadtmüller, R.; Nohl, H. *Biochem. Pharmacol.* **2005**, *69*, 1351.
2. Stolze, K.; Rohr-Udilova, N.; Rosenau, T.; Hofinger, A.; Kolarich, D.; Nohl, H. *Bioorg. Med. Chem.* **2006**, *14*, 3368.
3. Stolze, K.; Rohr-Udilova, N.; Rosenau, T.; Hofinger, A.; Nohl, H. *Bioorg. Med. Chem.* **2007**, *15*, 2827.
4. Stolze, K.; Rohr-Udilova, N.; Hofinger, A.; Rosenau, T. *Bioorg. Med. Chem.* **2008**, *16*, 8082.
5. Culcasi, M.; Rockenbauer, A.; Mercier, A.; Clément, J.-L.; Pietri, S. *Free Radical Biol. Med.* **2006**, *40*, 1524.
6. Villamena, F. A.; Rockenbauer, A.; Gallucci, J.; Velayutham, M.; Hadad, C. M.; Zweier, J. L. *J. Org. Chem.* **2004**, *69*, 7994.
7. Villamena, F. A.; Xia, S.; Merle, J. K.; Lauricella, R.; Tuccio, B.; Hadad, C. M.; Zweier, J. L. *J. Am. Chem. Soc.* **2007**, *129*, 8177.
8. Zhang, H.; Joseph, J.; Vasquez-Vivar, J.; Karoui, H.; Nsanzumuhire, C.; Martásek, P.; Tordo, P.; Kalyanaraman, B. *FEBS Lett.* **2000**, *473*, 58.
9. Dikalov, S.; Jiang, J.; Mason, R. P. *Free Radical Res.* **2005**, *39*, 825.
10. Chignell, C. F.; Kalyanaraman, B.; Sik, R. H.; Mason, R. P. *Photochem. Photobiol.* **1981**, *34*, 147.
11. Kirino, Y.; Ohkuma, T.; Kwan, T. *Chem. Pharm. Bull.* **1981**, *29*, 29.
12. Roubaud, V.; Lauricella, R.; Bouteiller, J. C.; Tuccio, B. *Arch. Biochem. Biophys.* **2002**, *397*, 51.
13. Dikalov, S. I.; Mason, R. P. *Free Radical Biol. Med.* **2001**, *30*, 187.
14. Stolze, K.; Udilova, N.; Nohl, H. *Biol. Chem.* **2002**, *383*, 813.
15. Stolze, K.; Udilova, N.; Rosenau, T.; Hofinger, A.; Nohl, H. *Biol. Chem.* **2003**, *384*, 493.
16. Olive, G.; Mercier, A.; LeMoigne, F.; Rockenbauer, A.; Tordo, P. *Free Radical Biol. Med.* **2000**, *28*, 403.
17. Zhao, H.; Joseph, J.; Zhang, H.; Karoui, H.; Kalyanaraman, B. *Free Radical Biol. Med.* **2001**, *31*, 599.
18. Weaver, J.; Tsai, P.; Pou, S.; Rosen, G. M. *J. Org. Chem.* **2004**, *69*, 8423.
19. Fréjaville, C.; Karoui, H.; Tuccio, B.; Le Moigne, F.; Culcasi, M.; Pietri, S.; Lauricella, R.; Tordo, P. *J. Med. Chem.* **1995**, *38*, 258.